buildings

MDPI

Article

Quantifying Multifactor Effects on Mud Cake Formation Risk for a Tunnel Boring Machine with the Analytical Hierarchy Process

Xiaobin Ding [1,2], Arnold Yuxuan Xie [3,*], Huitai Yang [2] and Shijia Li [4]

1 South China Institute of Geotechnical Engineering, South China University of Technology, Guangzhou 510641, China
2 School of Civil Engineering and Transportation, South China University of Technology, Guangzhou 510641, China
3 Department of Civil and Environmental Engineering, Western University, London ON N6A 3K7, Canada
4 Guangzhou Rail Transit Construction Supervision Co., Ltd., Guangzhou 510010, China
* Correspondence: yxie469@uwo.ca or w450198403@gmail.com

Abstract: Tunnel boring machines often encounter clogging during excavation in strata with rich clay content. The clogging can damage the cutterhead and interrupt excavation. Cutting tool clogging, also known as mud cake formation, has a strong effect on excavation work efficiency. While current studies are focusing on the mechanism of clogging, engineering practice still heavily relies on qualitative empirical judgement. To quantitatively assess the risk of mud cake formation, we carefully selected 22 influential parameters to reflect the effect of geological, machinal, and operational risk factors in the tunneling process and established a rubric for risk factor contributions using the analytical hierarchy process (AHP). The results imply the liquidity index, plasticity index, cutterhead torque, and total thrust force contribute to around 45% of the total influence on mud cake formation, while machinal factors are less influential than geological and operational factors. We verified the framework with a tunnel section from the Guangzhou Metro Line 22 that had mud cake formation reported. Rings labelled as high risk for mud cake formation by our framework concurred with those rings with mud cake actually observed. Project log and operational parameter variations were incorporated to explore the connection between mud cake formation and treatment.

Keywords: shield tunneling; clogging; mud cake; multifactor analysis; risk evaluation

Citation: Ding, X.; Xie, A.Y.; Yang, H.; Li, S. Quantifying Multifactor Effects on Mud Cake Formation Risk for a Tunnel Boring Machine with the Analytical Hierarchy Process. *Buildings* **2023**, *13*, 355. https://doi.org/10.3390/buildings13020355

Academic Editor: Ahmed Senouci

Received: 29 December 2022
Revised: 20 January 2023
Accepted: 22 January 2023
Published: 27 January 2023

1. Introduction

The tunnel boring machine (TBM) has been increasingly popular in urban underground constructions. The earth pressure balance tunnel boring machine (EPB-TBM) supports the earth pressure at the tunnel face by pressurized soil or fluid in the cutterhead to minimize the surrounding disturbance. When excavating in sticky ground, the pulverized geomaterials, namely muck, can adhere to the steel components, such as cutters and conveyor screws or bands [1]. The attached muck will solidify under the high pressure and high temperature clogging the TBM. Evidence shows the clogging cutterhead consumed energy six times higher than the normal energy per unit excavation [2].

Current studies on cutterhead clogging formation and mitigation concentrate on the clay–tool adhesion effect. Feinendegen et al., [3] designed a cone pull-out test to measure soil–steel adherence for clogging potential estimation. Zumsteg and Puzrin [4] developed a shear-plate apparatus to quantify the dispersing effect of chemical additives on tangential clay–tool adherence. Liu et al. [5] elucidated the electrochemical mechanism of dispersant on the Atterberg limit. Their findings concur with the cutterhead clogging risk evaluation chart from Hollmann and Thewes [6]. Attributing the clogging to grain size distribution, clayey mineral content, and water inflow, Thewes and Hollmann [7] proposed a more generalized version of the cutterhead clogging risk assessment regarding the Atterberg limit. They mentioned that the clogging at cutting tools, which is also known as mud cake, can induce clogging in the sieve and screw conveyor. In addition to earth pressure balance shield tunneling, Zhao et al. [8] discussed the effect of dispersant on mud cake formation prevention in slurry shield tunneling. Whereas, Fu et al. [9] introduced a temperature monitoring system for mud cake formation detection and demonstrated its application with a slurry shield tunneling project.

These research studies on mud cake formation and clogging either focus on specific cases of failure [2,9] or on lack of quantitative criterion [10,11]. The former can hardly be adapted to new tunneling projects due to the intrinsic variability of geomaterial and the uniqueness of machinal design, while the latter is susceptible to practitioners' subjective judgements. The prognosis of mud cake or cutterhead clogging still highly relies on experience in engineering practice, while advances in monitoring technology have provided real-time quantitative feedback of the TBM.

The formation of mud cake involves parameters from multiple aspects. The parameters can be classified into geological, machinal, and operational factors. Considering parameters from the three aspects and quantifying the contribution of involved parameters can not only take advantage of the rich diagnostic information from the TBM operation, but also elucidate the mechanism of mud cake formation from a field parameter perspective.

We carefully selected 22 parameters from the three categories then quantified their contribution to mud cake formation with a rubric by using the analytical hierarchy process (AHP) method to facilitate the preliminary evaluation of mud cake risk in engineering practice. The justification of parameter selections is presented in Section 2, followed by establishment of the AHP model in Section 3. Section 4 exhibits the model verification on a tunnel section with the circumstantial engineering records on mud cake encounter and mitigation. Section 5 summarizes the main findings of this study.

2. Background

2.1. Geological Condition

Viscous mineral particles have a significant effect on cutterhead clogging [12]. Clogging can occur in plastic and hard plastic clay strata, clayey sand strata, mudstone, muddy siltstone, and residual soil strata whose parent rock is granite, fully weathered rock strata, and strongly weathered rock strata, etc. These strata generally have small internal friction angles and large cohesion. The percentage of fine particles with grain size smaller than 0.075 mm are usually higher than 60% in these strata. It has been reported that the clogging potential increases significantly when the clayey mineral content exceeds 25% [13].

A series of tests and evaluation charts were established based on the Atterberg limit, i.e., liquid limit and plasticity limit, to correlate the clogging potential with soil consistency [7]. Underground water inflow can change stiff and hard clay with high plasticity into medium or soft clay during excavation. The soft clay will adhere to the cutting tools and solidify under the high pressure and temperature conditions. Burbaum and Sass [14] posit a fluid film around the fine particles inducing a microscopic surface tension force and macroscopic adhesion. The Atterberg limit is also a macroscopic measurement of the microscopic pore water tension properties.

In summary, we selected the mineral content, plasticity index, and liquidity index as geological parameters. Table 1 lists the specific value of them for risk level assessment.

2.2. Machinal Parameters

The opening rate of the cutterhead is crucial in mud cake formation [12]. Cutterheads with an opening rate beyond 33% generally have higher risk than those below 33% [13]. Wang [15] analyzed the EPB shield in sand strata quantitatively and proposed an equation to estimate the opening rate without muck lumping as shown in Equation (1).

$$\xi = \sqrt{\frac{\left|\frac{2c}{k_1} + (1+K_0)\gamma H \frac{\tan\varphi}{k_2}\right| 2L \cdot e_{\max}}{D(\mathrm{p}_0 - \mathrm{p}_\mathrm{a})}} \tag{1}$$

where ξ is the cutterhead opening rate in percentage, D is the cutterhead diameter in meters, p_0 and p_a are the lateral and active earth pressure on the tunnel face in kPa, respectively, c and φ are the soil cohesion and internal friction angle in kPa and degrees, respectively, K_0 is the dimensionless lateral earth pressure coefficient, γ is the average specific weight of the soil mass above the tunnel crown in N/m^3, H is the buried tunnel depth in meters, L is the length of the cutterhead in meters, e_{max} is the maximal muck discharge rate in percentage, and there are two empirical coefficients k_1 = 4.3, k_2 = 1.8.

Incompatible cutter spacing and height can lead to uneven stress distribution on the tool-soil interface accelerating cutter wear [16]. Excessive heat generated during abnormal wear will increase the risk of cutterhead clogging. The theoretical value for cutter spacing can be estimated by Equation (2), where [L] is the maximum distance for cutter inspection in meters; [δ] is the allowable cutter wear in millimeters, commonly 10–20 mm; v is the advance speed in centimeters per min; r is the installation radius of cutters in meters; K_{cw} is the cutter wear coefficient in millimeters per kilometer; n_d is the rotational speed of the cutterhead in rounds per minute [17]. Using cutters incompatible with the geological conditions can also result in a higher potential of mud cake formation. Disc cutters can reduce cutterhead wear in hard rock strata. Cutterheads can have larger opening rates and high excavation efficiency when equipped with scrapers in soft ground.

$$[L] = \frac{5[\delta]v}{\pi r K_{cw} n_d} \tag{2}$$

The disintegrated soil goes into the excavation chamber, where the mixing, muck discharge, and washing system also affect the clogging. A set of mixing blades are installed on the front and back wall of the excavation chamber. The blades on the front wall rotate together with the cutterhead, known as the active mixing blades, while those on the back wall are named the passive mixing blades as they are fixed. All these blades mix the muck and additives until the desired rheology is obtained. The muck is then exhausted by a screw conveyor. The ratio of the inlet length of the screw conveyor to the thickness of the excavation chamber, defined as the relative inlet length, determines the muck discharge efficiency. A screw conveyor with a longer inlet length discharges muck faster than that with a shorter inlet length. Consequently, the muck stays for a shorter time in the excavation chamber under high pressure so that the mud cake formation risk is lower. Additionally, a washing system that spouts high pressure water or slurry to the cutterhead can flush down the dirt on the cutterhead and cool it down to mitigate mud cake formation. The mixing blades, excavation chamber thickness, and inlet length of the screw conveyor are depicted in Figure 1.

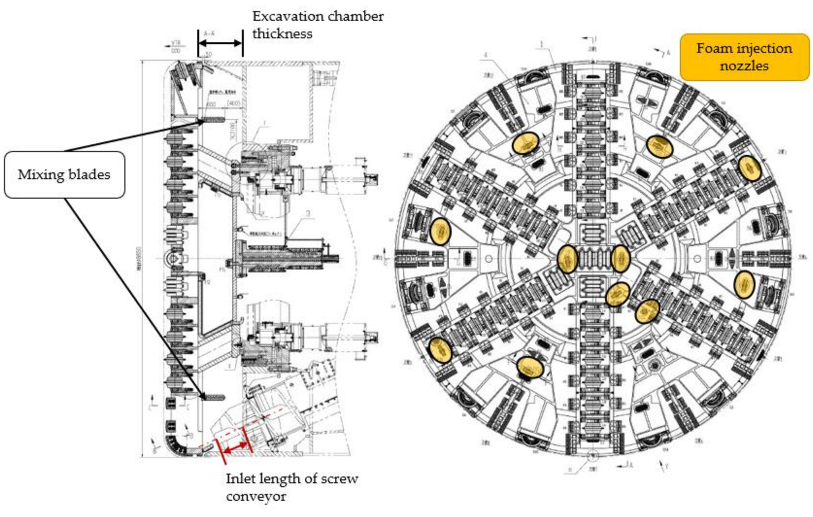

Figure 1. Illustration of mechanical components affecting mud cake formation risk in DZ187 shield machine.

In conclusion, the machinal factors of mud cake risk assessment include cutter spacing and penetration, cutter type, opening rate, the number of mixing blades, inlet length of the screw conveyor, and the washing system. The quantitative assessment of their risk level is listed in Table 1.

2.3. Operational Parameters

The operational parameters include the excavation mode, soil conditioning, and standby time. The excavation mode will result in various starting torques and muck levels. The cutterhead usually operates at a high starting torque in mixed strata, such as upper soil lower rock strata. The increase in torque and randomly distributed geology are conducive to an uneven friction force on the cutter-rock interface. Constant uneven friction force on the cutter will lead to abnormal cutter wear and generate enormous heat thus expediting mud cake formation [18].

Earth pressure balance shield tunneling usually adjusts the earth pressure in the excavation chamber by controlling the muck discharge rate. High pressure air is pumped into the excavation chamber to create an additional support pressure, known as the auxiliary air pressure balance mode [19,20]. It requires low permeability strata to implement this method. In this mode, the volume of muck is usually 1/2–2/3 of the excavation chamber and remaining part is filled with pressurized air, so that the torque and thrust are lower than the conventional earth pressure balance scheme due to the reduction in resistance from the muck. As the center area has a significantly high risk of mud cake formation, maintaining the muck volume at less than half of the excavation chamber can reduce the clogging risk. [13,21]

Excessive downtime is not trivial in mud cake formation. The downtime can occur in many situations, such as by removal of the launch segment lining. When the earth pressure balance shield is shut down, the muck in the excavation chamber begins to settle and build up pressure. During the process, the soil temperature often exceeds 50 °C and the pressure exceeds 0.1 MPa. As the soil temperature gradually decreases, the muck shrinks and forms a mud cake [6].

The mud cake formation starts with the spread of clay particles from the cutters. Mud cakes block the opening on the cutterhead so that the cutting soil cannot enter the excavation chamber. This results in a sharp increase in shield thrust and cutter frictional heat. The large amount of heat will not only promote a "sintering" effect of the mud cake, but also damage the cutterhead due to excessive thermal stress [22]. In this process, the increase of the cutterhead torque can be described by a third-degree polynomial function, while the excavation speed decreases exponentially [23]. In addition, the mud cake can block the foam opening at the center of the cutterhead, which significantly compromises the soil conditioning effect of the additives. This raises the risk of mud cake formation in the excavation chamber. The compacted mud cakes often decelerate the screw conveyor and even clog it.

Wang and Fu [24–26] correlated screw conveyor speed to earth pressure, cutterhead torque, total thrust, and excavation speed in the EPB-TBM. The correlations are illustrated in Equations (3) to (7). In Equations (3) and (7), p is the excavation chamber pressure in kPa; D is the tunnel diameter in m; δ is the surcharge pressure tunnel face in kPa; λ is the cutterhead opening rate in percentage; P_0 is the static earth pressure at the tunnel surface in kN; K is the quasi-stiffness in kPa/m; ΔS is the variation in advance distance in meters; k_e is the dimensionless effective soil discharge ratio; η is a dimensionless parameter related to the soil properties and soil discharge efficiency; k is a parameter related to the form of the screw machine in newtons per round; γ_0 is the natural specific density of the soil in N/m^3; N is the rotational speed of the screw conveyor in rounds per minute (rpm); v is the advance speed in meters per minute (m/min). In Equation (4), F is total thrust force and F_0 is the total resistance on the tunnel face, while other parameters have identical definitions as Equations (3) and (7).

In Equation (5), T is the cutterhead torque in kNm; f is the dimensionless friction coefficient; p_0 is the original lateral soil pressure in kPa, Δp_2 is the additional pressure in kPa caused by the cutter advances, ξ is the cutterhead opening rate in percentage. The coefficient α depends on the pattern of opening on the cutterhead. It equals 1 for the spoke type cutterheads and ranges from 1 to 1.5 for the plate type ones. The terms c and φ are the soil cohesion and internal friction angle in kPa and degrees, respectively; D is the diameter of the cutterhead in meters; v is the advance speed in m/min; w is the rotational speed of the cutterhead in rounds per minute; γ is the specific density of soil in kN/m^3; H_0 is the buried depth of the mixing blades in meters; D_b and L_b are the diameter and length of the mixing blades in meters; R_b is the distance from the mixing blades to the cutterhead center in meters; f' is the dimensionless soil–tool friction coefficient [27]; n is the number of mixing blades. In Equation (6), A is an empirical coefficient, which is 20 for clayey soil, 35 for silty soil, 30 for sandy soil, and 25 for gravel, while d is the diameter of the screw conveyor in meters.

$$p\frac{\pi D^2}{4}\left[1+\frac{\delta}{p}(1-\lambda)\right] = P_0 + K\Delta S - K\left(\frac{4k_e\eta k\Delta S}{\gamma_0\pi D^2}\right)\frac{N}{v} \tag{3}$$

$$F = (F_0 + P_0 + K\Delta S) - K\left(\frac{4k_e\eta k\Delta S}{\gamma_0\pi D^2}\right)\frac{N}{v} \tag{4}$$

$$T = \frac{\pi f(2p_0+\Delta p_2)(1-\xi^\alpha)D^3}{12} + \left|p_0\tan^2\left(\frac{\pi}{4}+\frac{\varphi}{2}\right) + 2c\tan\left(\frac{\pi}{4}+\frac{\varphi}{2}\right)\right|\frac{D^2 v}{8w} + \sum_n \gamma H_0 D_b L_b R_b f' \tag{5}$$

$$N = \frac{A}{\sqrt{d}} \tag{6}$$

$$\frac{N}{v} = \frac{\gamma_0\pi D^2}{4k_e\eta k\Delta S} \tag{7}$$

Soil conditioning is an important tool for mud cake prevention and the commonly used additives are foam, bentonite, and epoxy resin. They can improve the fluidity and cohesiveness of the soil to give a "plastic flow state" [28]. Foam additives, for example, permeate the pores of the clay particles and reduce the adhesion between them. This improves the "compatibility" and "plasticity" of the soil and reduces the risk of mud cake formation. The main factors influencing the effectiveness of foam additives include the foam injection ratio (FIR), the foaming expansion ratio (FER), and the foam half-dissipation time. Foam additives with higher FER and longer half-dissipation time produce more stable foam and have a better conditioning effect. At the same time, the soil and cutterhead torque at the tunnel face decreases accordingly as the additive injection ratio increases. Ye et al. [10] derived a relationship between the foam injection ratio (FIR) and water content (w) from the slump and fluidity index of the soil, which is a valuable guideline for cutterhead clogging prevention.

Temperature also shows a dominant promoting effect on mud cake formation. Cutter and muck temperature control are an approach for mud cake prevention [9]. The temperature of the muck is usually 28–31 °C. When the temperature exceeds 35 °C, the possibility of mud cake formation rises significantly [21].

In summary, 12 parameters were selected to reflect the operational influence on mud cake formation. These factors are listed in Table 1 as d11 to d22 with the corresponding quantitative risk level assessment criteria.

Table 1. Rubric for risk level assessment.

Risk Factor \ Level of Risk	High Risk (100–75)	Medium Risk (75–50)	Low Risk (50–25)	Risk-Free (25–0)
d1 clay mineral content	>25% and FPC [a] >60%	15~25% and FPC > 30%	15~10%	<10%
d2 plasticity index	>17	10~17	6~10	<6
d3 liquidity index	0.385~0.667	−0.6 to 0.385	0.667~1	>1 or <−0.6
d4 cutter spacing error [b]	>50%	25%–50%	10%–25%	<10%
d5 cutter height difference	<20 mm	20~40 mm	40~60 mm	>60 mm
d6 strata compatibility of cutter types	Not compatible at all	Slightly compatible	Partially compatible	Custom-built
d7 cutterhead opening rate	<33% or <75% T_0 [c]	33~38% or 75~84% T_0	38~45% or 85~100% T_0	>45% or >T_0
d8 number of mixing blades	<4	4~6	6~8	>8
d9 relative inlet length of screw conveyer	<0.25	0.25~0.5	0.5~0.75	>0.75
d10 washing system	Not available	No central nozzle	More than 6 nozzles	Over 10 nozzles with central nozzles
d11 starting torque exceeding ratio [d]	>25%	10~25%	0~10%	0%
d12 muck level/chamber height	>2/3	1/2~2/3	>1/2	0
d13 downtime	>12h or >6 T_{se} [e]	3~6 T_{se}	2~3 T_{se}	=T_{se}
d14 excavation chamber pressure	>1.6$max\{T_0,T_e\}$ [f]	(1.4~1.6)$max\{T_0,T_e\}$	(1.1~1.4)$max\{T_0,T_e\}$	<1.1$max\{T_0,T_e\}$
d15 cutterhead torque	>1.5$max\{T_0,T_e\}$	(1.3~1.5)$max\{T_0,T_e\}$	(1.1~1.3)$max\{T_0,T_e\}$	<1.1$max\{T_0,T_e\}$
d16 total thrust force	>1.5$max\{T_0,T_e\}$	(1.3~1.5)$max\{T_0,T_e\}$	(1.1~1.3)$max\{T_0,T_e\}$	<1.1$max\{T_0,T_e\}$
d17 advance speed	<0.75$max\{T_0,T_e\}$	(0.75~0.85)$max\{T_0,T_e\}$	(0.85~0.95)$max\{T_0,T_e\}$	>0.95$max\{T_0,T_e\}$
d18 conveyor screw rotational speed	<0.75$max\{T_0,T_e\}$	(0.75~0.85)$max\{T_0,T_e\}$	(0.85~0.95)$max\{T_0,T_e\}$	>0.95$max\{T_0,T_e\}$
d19 foam injection ratio exceeding rate [g]	25%	15%	5%	0
d20 foam expansion ratio	<15	15~20	20~30	>30
d21 foam half-dissipation time	<4 min	4~6 min	6~8 min	>8 min
d22 muck temperature	>38 °C	35~38 °C	31~35 °C	28~31 °C

Note: a. FPC: fine particle content. Fine particles have size smaller than 0.075 mm; b. The error between actual and theoretical values from Equation (2); c. T_0: theoretical value from Equation (1); d. The error rate between actual and theoretical values from Equations (3)–(7); e. T_{se}: segment erection time; f. T_0, T_e denote the theoretical or empirical value of the corresponding term, respectively. g. Exceeding rate = 100% × {[(actual value)/(theoretical boundary value in [10])] − 1}.

3. Mud Cake Formation Risk Evaluation Model

There is an enormous number of influential parameters for mud cake formation. The formation mechanism is intricate and subject to sophisticated interaction among the parameters. The importance of these parameters is diverse, so it is necessary to conduct individual analysis on each parameter. The analytical hierarchy process (AHP) fulfills the objective of hierarchical and quantitative evaluation on the mud cake formation risk. According to the rubrics in Table 1, we demonstrate the risk importance quantification using AHP.

3.1. Analytical Hierarchy Process (AHP)

The method starts from picking a goal (R), which is the probability of mud cake formation in our case, let s_i, s_j (i, j = 1, 2, ..., n) be the influential factors of the goal. The relative importance of influential factor s_i to s_j, denoted as s_{ij}, can quantified by the 1–9 scale shown in Table 2. All the s_{ij}-s can then compose the R-S pairwise comparison matrix $\boldsymbol{P}$, the maximal eigenvalue λ_{max}, and the corresponding eigenvector $\boldsymbol{w}$ of matrix $\boldsymbol{P}$. The i-th element of the eigenvector $\boldsymbol{w}$, denoted as w_i, is the importance weight of the i-th factor s_i to the goal R.

It is necessary to check the consistency of the comparison matrix. If a comparison matrix suggests factor A > B and B > C, there should not be inconsistent weights suggesting C > A. This is done mathematically by the equation in Step 3, Figure 2, where CI is the consistency index, λ_{max} is the maximum eigenvalue, n is the number of evaluated criteria, RI is the random consistency index with value according the Table in Step 3 of Figure 2. CR is the ratio CI to RI. When CR < 10% or CI = 0, the matrix P satisfies the consistency requirement. If the consistency check fails, one should revise the parameters s_{ij} in the pairwise comparison matrix $\boldsymbol{P}$.

Table 2. Scale for pairwise comparisons. Intensities of 2 4, 6, and 8 are used to express intermediate cases. Decimal intensities, e.g., 1.1, 1.2, 1.3 can be used to distinguish elements with similar importance.

Intensity of Importance	Definition	Explanation
1	Equal Importance	Two elements contribute equally to the objective.
3	Moderate Importance	One element slightly contributes more than the other one.
5	Strong Importance	One element strongly contributes more than the other
7	Very Strong Importance	One element dominates between the two.
9	Extreme Importance	One element contributes so much that the other one is negligible

A global weight vector $\boldsymbol{W}$ can be obtained by stacking the local weight vectors $w_{\text{R-S}}$ of each layer. Specifically, the local weight vector of the current level multiplies the corresponding weight item in the previous level iteratively to distribute the contributions from the goal (R) to the bottom factors through the hierarchy.

The dot product of the global weight vector $\boldsymbol{W}$ and the quantitative input vector $\boldsymbol{F}$ returns the score S, a single value from 0 to 1, that indicates the degree of approval of the input combination to the goal.

Figure 2 summarizes the AHP in four steps. The application of AHP on mud cake formation risk evaluation will be elaborated in the next section.

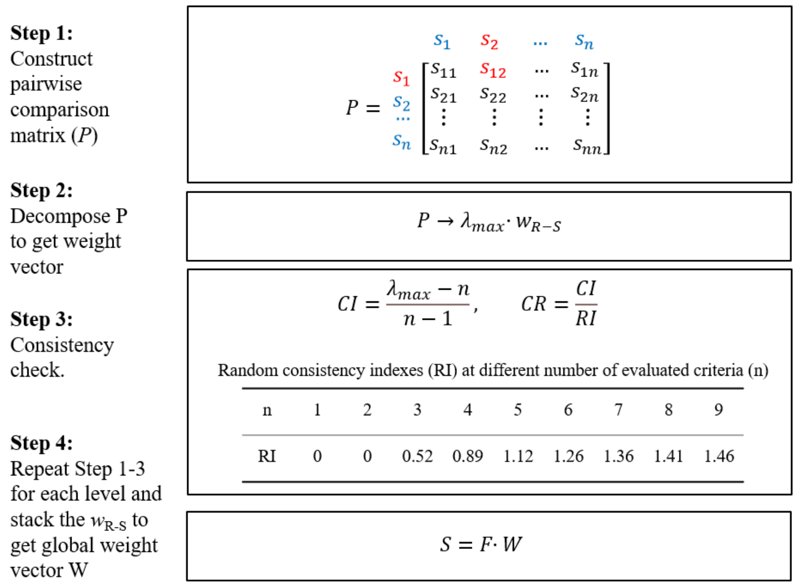

Figure 2. Framework to quantify the importance of influential factors with analytical hierarchy process (AHP) method. s_i is the i-th factor candidate to the goal, and s_{ij} denotes the relative importance of factor i to j according to Table 2. λ_{max} and $w_{\text{R-S}}$ are the maximum eigenvalue and corresponding eigenvector, respectively. S is a single value indicator from dot products of input vector F and global weight vector W.

3.2. Model Establishment

Based on the previous analysis of mud cake formation risk factors, factors affecting mud cake formation can be categorized as geological b1, machinal b2, or operational b3. The comparison matrix between mud cake formation risk a to factors b, denoted as $\boldsymbol{P}_{\text{a-b}}$, is shown in Table 3. According to Step 3 in Figure 2, the maximum eigenvalue λ_{max} = 3.0092 and the corresponding eigenvector $w_{\text{a-b}}$ = [0.297, 0.164, 0.539] are obtained. Consistency test results are CI = 0.0046, CR = 0.00885 < 0.1 indicating matrix $\boldsymbol{P}_{\text{a-b}}$ satisfies the consistency requirement.

Table 3. Comparison matrix and weight for secondary level.

	Geological Factors	Machinal Factors	Operational Factors	Weight (w_i)
Geological factors	1	2	1/2	0.297
Machinal factors	1/2	1	1/3	0.164
Operational factors	2	3	1	0.539

There are more machinal (b2) and operational (b3) factors than geological (b1) ones. To facilitate understanding of the hierarchical importance of mud cake formation, we set the tertiary level (c1–c7) analysis after the secondary level (b2, b3), and set the specific risk factors as quaternary level (d4–d22). The hierarchy of AHP is shown in Table 4. The comparison matrices and corresponding CI CR for secondary (b),tertiary (c), and quaternary level (d) are listed in Appendix A.

Table 4 lists the hierarchy of the influential factors in mud cake formation together with the quantified importance, viz., their local and global weights. Figure 3 visualizes the global weights illustrating that geological and operational factors have more significant influence on mud cake formation. Specifically, plasticity index (d2), liquidity index (d3), cutterhead torque (d15), and total thrust force (d16) show prominent effects. The four factors contribute a total weight value of 44.67%, nearly half of the 22 parameters. The cutterhead opening rate (d7) and muck temperature (d22) exhibit a nontrivial contribution with weight values of 5.27% and 6.42%, respectively.

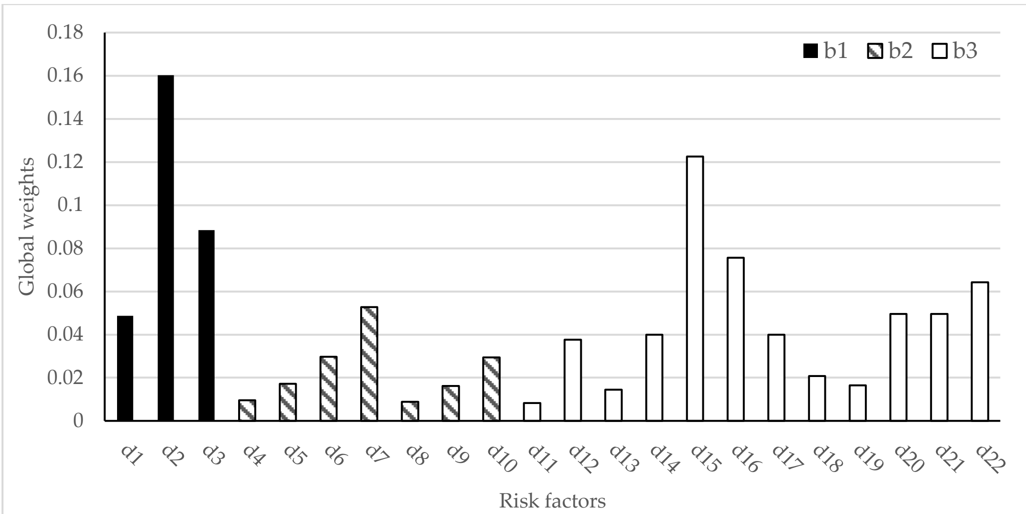

Figure 3. Bar chart of global weights of risk factors. d1–d22 indicate the risk factors and b1–b3 imply secondary factors in Table 4. Weights of d2 plasticity index, d3 liquidity index, d15 cutterhead torque, and d16 cutter thrust force surpass other factors significantly.

Table 4. Weight of factors in different levels (secondary, tertiary, quaternary) retrieved from AHP analysis on mud cake formation. Local weight is the weight among other parameters in the same level. Global weight implies the total contribution to the primary factor, mud cake formation.

Secondary Factors	Local/Global Weights	Tertiary Factors	Local Weights	Quaternary Factors/Risk Factors	Local Weights	Global Weight
b1 Geological factors	0.2973	——		d1 clay mineral content	0.1638	0.0487
				d2 plasticity index	0.539	0.1602
				d3 liquidity index	0.2972	0.0884

Table 4. *Cont.*

Secondary Factors	Local/Global Weights	Tertiary Factors	Local Weights	Quaternary Factors/Risk Factors	Local Weights	Global Weight
b2 Machinal factors	0.1638	c1 Cutters	0.6667	d4 cutter spacing error	0.0883	0.0096
				d5 cutter height difference	0.1575	0.0172
				d6 Strata compatibility of cutter types	0.2718	0.0297
				d7 Cutterhead opening rate	0.4824	0.0527
		c2 Not cutters	0.3333	d8 Number of mixing blades	0.1638	0.0089
				d9 Relative inlet length of screw conveyer	0.2973	0.0162
				d10 Washing system	0.539	0.0294
b3 Operational factors	0.539	c3 Excavation mode	0.1121	d11 Starting torque exceeding ratio	0.1373	0.0083
				d12 Muck level/chamber height	0.6232	0.0376
				d13 Downtime	0.2395	0.0145
		c4 Excavation parameters	0.5541	d14 Excavation chamber pressure	0.1336	0.0399
				d15 Cutterhead torque	0.4101	0.1225
				d16 Total thrust force	0.2531	0.0756
				d17 Advance speed	0.1336	0.0399
				d18 Conveyor screw rotational speed	0.0696	0.0208
		c5 Soil conditioning	0.2148	d19 Foam injection ratio exceeding rate	0.1429	0.0165
				d20 Foam expansion ratio	0.4286	0.0496
				d21 Foam half-dissipation time	0.4286	0.0496
		c6 Temperature control	0.1191	d22 Muck temperature	1	0.0642

4. Case Study

4.1. Mud Cake Risk Analysis

Mud cakes were found from ring#8 to #17 during excavation of the Guangzhou metro line 22, Qifu to Panqi section. The crew observed an abnormal operational parameter pattern and took various mitigation actions. The problem had not been compromised and eventually a manual inspection took place. The tunneling section used the DZ187 shield machine from the China Railway Construction Corporation with a cutterhead diameter of 8.8 m. The cutterhead had an opening rate of 35%. It was equipped with 6 center cutters, 35 face cutters, 12 gauge cutters, and 76 scrapers. The disc cutters and scrapers were 160 mm and 115 mm high, respectively. The cutter height difference was 45 mm. There were 9 foam nozzles, 6 active mixing blades, and 9 passive mixing blades. The cutterhead layout is depicted in Figure 1.

The section had a burial depth of 11.6 m in mix ground conditions. The tunnel crown near the launching area was in backfill with sandy clay strata. The tunnel wall was in sandy clay. The tunnel invert was in fully weathered mixed granite. The soil was sticky, and the content of fine particles exceeded 70%, which is conducive for mud cake formation. When the TBM was shutdown at Ring#17, it encountered strongly weathered mixed granite with sporadic medium weathered rock blocks. Once saturated, the strongly weathered granite disintegrated rapidly.

According to the construction log, the cutterhead was in the initial trial excavation stage. Potential mud-cake-prone factors during the shield tunneling process included full chamber excavation, constantly high excavation chamber pressure, incompatible mix proportion and injection rate of additives, and long downtime.

Following the rubric in Table 1, we obtain the risk assessment input vector at Ring#17 F_{17} = [70, 70, 66, 81, 44, 75, 68, 20, 48, 30, 89, 93, 52, 83, 97, 75, 100, 100, 90, 67, 83, 80]. The dot product of F_{17} and weight vector W, whose elements are the global weights in the last column of Table 4, return 75.6 > 75. The excessive risk value implies ring#17 has high potential for mud cake formation. This is also the maximal risk value within the tunnel section from Ring#4 to Ring#20.

4.2. Shield Tunneling Process Analysis

Figure 4 shows the changes of the total thrust and cutterhead torque of the shield in the mud cake formation section and the main treatment after observing the abnormal shield parameters. The geological conditions of the tunnel section are similar, so the theoretical thrust and torque are constant values. The excavation speed, rotational speed, and excavation chamber pressure are shown in Figure 5.

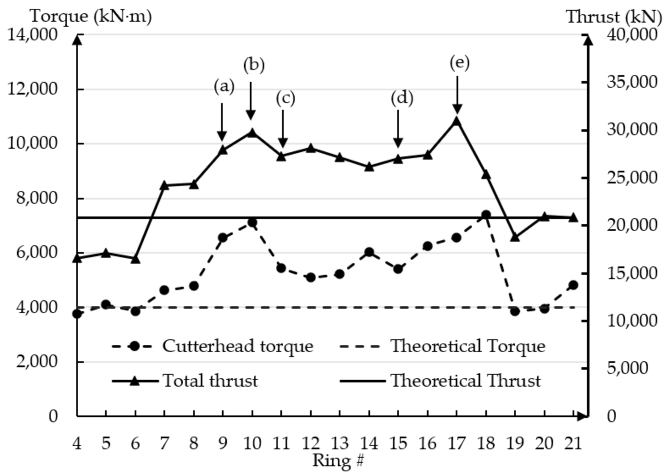

Figure 4. The total thrust force and cutterhead torque variation of the studied tunnel section. Theoretical torque and thrust are 4012 kNm and 20,783 kN, respectively. Both are calculated from Equations (3)–(7). Arrows indicate mud cake mitigations: (**a**) modify foam ratio, (**b**) increase water and dispersant, (**c**) auxiliary air pressure support, (**d**) dispersant soaking, and (**e**) open chamber inspection.

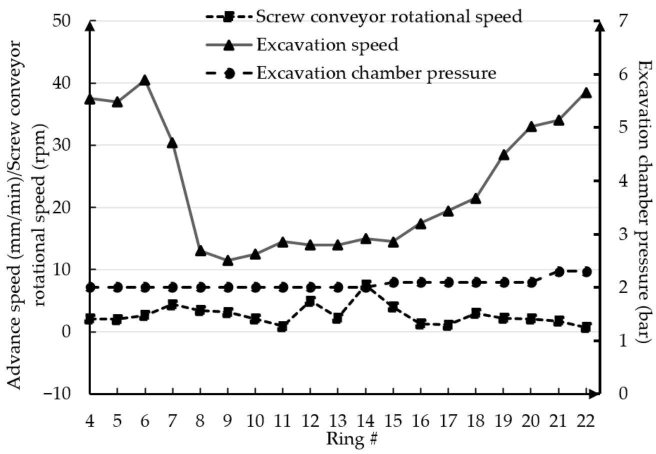

Figure 5. Excavation speed, screw conveyor rotational speed, and excavation chamber pressure variation of the studied tunnel section.

The initial thrust force stays around 17,000 kN. The cutterhead torque gradually increased from 3000 to 4000 kNm. When the cutterhead reached ring#8, the total thrust force and cutterhead torque exhibited an abrupt increase. The cutterhead torque rose from 4491 to 8757 kNm for the next two rings. In Figure 5, the excavation chamber pressure increases, and the excavation speed slows down from ring#8. While the log reported the temperature of discharged muck reached 30 °C, the muck from the screw conveyor has poor mobility, and the foam injection nozzle at the center of the cutterhead appears to be blocked. These variation on operational parameters and muck properties imply mud cake formation. It was found that the additive foam with a foam ratio of 2:98 could not achieve the desirable soil conditioning effect. Thus, they changed the foam ratio to 3.5:96.5 from Ring#9 to enhance the soil conditioning effect.

After modifying the foam ratio, the shield thrust and cutterhead torque kept increasing in the 10th ring. The excavation speed fluctuated. The crew took further action, such as increasing the amount of water and foam, reducing the rotational speed, and adding dispersant. These measures helped bring down the thrust force and torque at Ring #11, but the 58 °C muck from screw conveyor indicated clogging still existed. Thus, they accelerated the muck discharge rate and activated the auxiliary air pressure balance mode.

Switching to auxiliary air pressure balance mode, the cutterhead torque and thrust force decreased in Ring#12 and #13 but rose abruptly in Ring #14 accompanied by a drop in excavation speed. The crew responded with dispersion-type foam agent soaking.

The total thrust force and cutterhead torque continued to increase after the soaking until Ring#17. The mud cake could not be compromised by conventional additives anymore. There was a great risk of cutterhead damage if the excavation continued. Therefore, the cutterhead was stopped at Ring#17 for maintenance.

It is evident that cutterhead torque and thrust force are key parameters for mud cake formation evaluation. The two parameters varied in a similar trend. They were both much higher than the theoretical value after mud cake occurred. Meanwhile, the excavation chamber pressure showed a smooth variation to maintain the stability at the tunnel face.

To determine the risk of mud cake formation, a preliminary judgment should be made according to the geological conditions, which are the basis for mud cake formation. First, check if the cutterhead mainly encounters mud-cake-prone strata. Then, the possibility of mud cake formation should be further analyzed according to the clay mineral particle content, consistency coefficient, and plasticity index of these strata.

The second type of factors is machinal, i.e., the design of the cutterhead. A customized cutterhead could effectively reduce the risk of mud cake formation even in mud-cake-prone strata. A critical machinal factor affecting the mud cake formation is the opening rate in the center area of the cutterhead. Other machinal factors that lead to high risk of mud cake formation are improper cutter layout, insufficient height difference of the cutters, lack of mixing blades, a small excavation chamber, a short inlet of the screw conveyor, and no jet washing system.

Once the excavation initiates, the operational factors partake in the formation of mud cake. The excavation chamber pressure is an important operational factor as excessive pressure can compact muck in the excavation chamber making it hard to discharge which eventually results in mud cake. If the height of the muck level in the excavation chamber is lower than the center of the cutterhead, the possibility of mud cake formation in the shield is negligible, so the use of the auxiliary air pressure mode in tunneling can effectively prevent mud cake formation. The injection of additives, such as foam and other additives, can effectively reduce the probability of mud cake formation. Whereas, when the existence of mud cake is already confirmed and key operational parameters, such as high muck temperature, have remained abnormal for a long time, the excavation should be interrupted timely for cutterhead inspection.

5. Conclusions

Excavation in strata with clay content leads to high risk of the TBM clogging that can interrupt the excavation and damage the cutterhead. Mud cake formation is a common cause of cutterhead clogging. While many studies have investigated the mechanism of clogging, engineering practice still heavily relies on qualitative empirical judgement. We established a quantitative model for mud cake formation risk assessment for the tunnel boring machine using the analytical hierarchy process (AHP). We demonstrated the efficacy of the model with a tunnel section of the Guangzhou Metro Line 22.

We quantified the importance of 22 influential parameters covering geology, machines, and operation. The weights of the risk evaluation vector suggest that the plasticity index (d2), liquidity index (d3), cutterhead torque (d15), and the total thrust force (d16) have predominant importance in mud cake formation. Together they contribute nearly half of the global weights from risk factors for mud cake formation. Generally, the machinal factors reflected by the selected parameters are not comparable to the geological and operational factors.

The case study further supports the results from AHP analysis that cutterhead torque is a key parameter for mud cake formation evaluation. Cutterhead torque increases abruptly during the generation of mud cake and shows a consistent trend with the thrust force, while the excavation speed slows down and fluctuates. Auxiliary air pressure balanced tunneling can effectively prevent mud cake formation. Injecting additives, such as foam agents, can also compromise the risk of mud cake formation. Once the existence of mud cake is confirmed, the excavation should be stopped to eliminate the mud cake as quickly as possible.

Author Contributions: Conceptualization and methodology, X.D.; formal analysis, writing, A.Y.X.; investigation, validation, H.Y.; resources, S.L. All authors have read and agreed to the published version of the manuscript.

Funding: This study was supported by National Natural Science Foundation of China (Grant No. 41827807), Science Foundation of Guangdong Provincial Key Laboratory of Modern Civil Engineering Technology 2021B1212040003.

Institutional Review Board Statement: Not applicable.

Informed Consent Statement: Not applicable.

Data Availability Statement: Data available upon reasonable request due to commercial restrictions.

Conflicts of Interest: The authors declare no conflict of interest.

Appendix A

Pairwise comparison matrix for a-b level was introduced in Section 3.2. All the other pairwise comparison matrices are listed here. For definition of secondary, tertiary, and quaternary levels see Table 4.

Table A1. Pairwise comparison matrix for tertiary level machinal factors (b2-c). λ_{max} = 2; CR = 0; CI = 0.

	Cutters	Not Cutters	Weights
Cutters	1	2	0.666667
Not cutters	1/2	1	0.333333

Table A2. Pairwise comparison matrix for tertiary level operational factors (b3-c). λ_{max} = 4.0155; CR = 0.00581; CI = 0.00516819.

	Excavation Mode	Excavation Parameters	Soil Conditioning	Temperature Control	Weights
Excavation mode	1	1/5	1/2	1	0.112065
Excavation parameters	5	1	3	4	0.554076
Soil conditioning	2	1/3	1	2	0.214785
Temperature control	1	1/4	1/2	1	0.119075

Table A3. Pairwise comparison matrix for quaternary level geological factors (b1-d) λ_{max} = 3.0092; CR = 0.00885; CI = 0.00460136.

	Clay Mineral Content	Plasticity Index	Liquidity Index	Weights
clay mineral content	1	1/3	1/2	0.163781
plasticity index	3	1	2	0.538961
liquidity index	2	1/2	1	0.297258

Table A4. Pairwise comparison matrix for quaternary level cutters machinal factors (c1-d) λ_{max} = 4.01452; CR = 0.00544; CI = 0.00484032.

	Cutter Spacing Error	Strata Compatibility of Cutter Types	Cutter Height Difference	Cutterhead Opening Rate	Weights
cutter spacing error	1	1/3	1/2	1/5	0.0882873
strata compatibility of cutter types	3	1	2	1/2	0.271798
cutter height difference	2	1/2	1	1/3	0.157508
cutterhead opening rate	5	2	3	1	0.482407

Table A5. Pairwise comparison matrix for quaternary level not cutters machinal factors (b2-c) λ_{max} = 3.0092; CR = 0.00885; CI = 0.00460136.

	Relative Inlet Length of Screw Conveyer	Number of Mixing Blades	Washing System	Weights
relative inlet length of screw conveyer	1	2	1/2	0.297258
number of mixing blades	1/2	1	1/3	0.163781
washing system	2	3	1	0.538961

Table A6. Pairwise comparison matrix for quaternary level operational excavation mode factors (c3-d) λ_{max} = 3.01829; CR = 0.01759; CI = 0.00914735.

	Muck Level/Chamber Height	Downtime	Starting Torque Exceeding Ratio	Weights
muck level/chamber height	1	3	4	0.623225
downtime	1/3	1	2	0.239488
starting torque exceeding ratio	1/4	1/2	1	0.137288

Table A7. Pairwise comparison matrix for quaternary level excavation parameters operational factors (c4-d) λ_{max} = 5.0182; CR = 0.00406; CI = 0.00455015.

	Excavation Chamber Pressure	Cutterhead Torque	Total Thrust Force	Advance Speed	Conveyor Screw Rotational Speed	Weights
excavation chamber pressure	1	1/3	1/2	1	2	0.133603
cutterhead torque	3	1	2	3	5	0.410053
total thrust force	2	1/2	1	2	4	0.253122
advance speed	1	1/3	1/2	1	2	0.133603
conveyor screw rotational speed	1/2	1/5	1/4	1/2	1	0.0696185

Table A8. Pairwise comparison matrix for quaternary level soil conditioning operational factors (c5-d) $\lambda_{max} = 3$; CR = 0; CI = -1.11022×10^{-15}.

	Foam Injection Ratio Exceeding Rate	Foam Expansion Ratio	Foam Half-Dissipation Time	Weights
foam injection ratio exceeding rate	1	1/3	1/3	0.142857
foam expansion ratio	3	1	1	0.428571
foam half-dissipation time	3	1	1	0.428571

References

1. Feinendegen, M.; Ziegler, M.; Spagnoli, G.; Fernández-Steeger, T. Evaluation of the Clogging Potential in Mechanical Tunnel Driving with EPB-Shields. In *Proceedings of the 15th European Conference on Soil Mechanics and Geotechnical Engineering*; IOS Press: Amsterdam, The Netherlands, 2011; pp. 1633–1638.
2. Bilgin, N. An Appraisal of TBM Performances in Turkey in Difficult Ground Conditions and Some Recommendations. *Tunn. Undergr. Space Technol.* **2016**, *57*, 265–276. [CrossRef]
3. Feinendegen, M.; Ziegler, M.; Weh, M.; Spagnoli, G. Clogging during EPB-Tunnelling: Occurrence, Classification and New Manipulation Methods. In Proceedings of the ITA-AITES World Tunnel Congress, Helsinki, Finland, 21–26 May 2011; Volume 299, pp. 767–776.
4. Zumsteg, R.; Puzrin, A.M. Stickiness and Adhesion of Conditioned Clay Pastes. *Tunn. Undergr. Space Technol.* **2012**, *31*, 86–96. [CrossRef]
5. Liu, P.; Wang, S.; Ge, L.; Thewes, M.; Yang, J.; Xia, Y. Changes of Atterberg Limits and Electrochemical Behaviors of Clays with Dispersants as Conditioning Agents for EPB Shield Tunnelling. *Tunn. Undergr. Space Technol.* **2018**, *73*, 244–251. [CrossRef]
6. Hollmann, F.S.; Thewes, M. Assessment Method for Clay Clogging and Disintegration of Fines in Mechanised Tunnelling. *Tunn. Undergr. Space Technol.* **2013**, *37*, 96–106. [CrossRef]
7. Thewes, M.; Hollmann, F. Assessment of Clay Soils and Clay-Rich Rock for Clogging of TBMs. *Tunn. Undergr. Space Technol.* **2016**, *57*, 122–128. [CrossRef]
8. Zhao, Y.; Yang, T.; Zhang, P.; Xu, H.; Zhou, J.; Yu, Q. Method for Generating a Discrete Fracture Network from Microseismic Data and Its Application in Analyzing the Permeability of Rock Masses: A Case Study. *Rock Mech. Rock Eng.* **2019**, *52*, 3133–3155. [CrossRef]
9. Fu, J.; Xia, Y.; Lan, H.; Wu, D.; Lin, L. A Case Study on TBM Cutterhead Temperature Monitoring and Mud Cake Formation Discrimination Method. *Sci. Rep.* **2021**, *11*, 19983. [CrossRef]
10. Ye, X.; Wang, S.; Yang, J.; Sheng, D.; Xiao, C. Soil Conditioning for EPB Shield Tunneling in Argillaceous Siltstone with High Content of Clay Minerals: Case Study. *Int. J. Geomech.* **2017**, *17*, 05016002. [CrossRef]
11. Frenzel, C. Disc Cutter Wear Phenomenology And Their Implications On Disc Cutter Consumption For TBM. In Proceedings of the 45th US Rock Mechanics/Geomechanics Symposium, San Francisco, CA, USA, 26 June 2011.
12. Burbaum, U. Adhäsion Bindiger Böden an Werkstoffoberflächen von Tunnelbohrmaschinen. Ph.D. Thesis, Technische Universität, Darmstadt, Germany, 2009.
13. Yan, H. Mechanism of formation and prevention measures of cutter mud cake in shield tunnel construction. *Mod. Tunn. Technol.* **2007**, *44*, 24–27. (In Chinese)
14. Burbaum, U.; Sass, I. Physics of Adhesion of Soils to Solid Surfaces. *Bull. Eng. Geol. Environ.* **2017**, *76*, 1097–1105. [CrossRef]
15. Hong-Xin, W. Type Selection of the Head Aperture Ratio of EPB Shield Cutter Heads and Adaptability to Stratum Characteristics. *China Civ. Eng. J.* **2010**, *43*, 88–92. (In Chinese)
16. Farrokh, E. Layout Design Specifications of Hard-Rock TBM Cutterheads at Maximum Cutter Penetration and TBM Advance. *Arab J Geosci* **2021**, *14*, 2049. [CrossRef]
17. Zhao, L.; Chen, Y.; Liu, F. Compound Shield Tool Arrangement Analysis and Research. *Mod. Tunn. Technol.* **2012**, *49*, 32–37. (In Chinese) [CrossRef]
18. Fu, X.; Tao, M.; Chen, Z.; Qingyang, L.; Yongmin, W. Causes and preventive measures for mud cake formation on shield machine cutter in composite strata. *Chin. J. Undergr. Space Eng.* **2020**, *16*, 864–869. (In Chinese)
19. Jenny, R.J. Compressed Air Use in Soft Ground Tunneling. *J. Constr. Eng. Manag.* **1983**, *109*, 206–213. [CrossRef]
20. Wang, S.; Liu, P.; Gong, Z.; Yang, P. Auxiliary Air Pressure Balance Mode for EPB Shield Tunneling in Water-Rich Gravelly Sand Strata: Feasibility and Soil Conditioning. *Case Stud. Constr. Mater.* **2022**, *16*, e00799. [CrossRef]
21. Guodong, Z.; Yinbin, Y. Causes of Cutter Center Body Mud Cake and Its Prevention and Control Measures. *Railw. Constr. Technol.* **2017**, 69–72. (In Chinese)
22. Li, X.; Yi, Y. Structural coupling analysis of mud and water shield blade heat considering frictional heat effect. *J. Civ. Eng.* **2020**, *53*, 20–24. (In Chinese) [CrossRef]
23. Yong, F.; Kai, W.; Liming, T.; Pengcheng, L.; Ruyong, D. Experimental study on clogging of cutterhead for panel earth-pressure-balance shield tunneling in cohesive strata. *Chin. J. Geot. Eng.* **2020**, *42*, 1651–1658. (In Chinese) [CrossRef]

24. Wang, H. Earth Pressure Balance Shield Blade Torque Calculation and Its Relationship with Shield Construction Parameters. *J. Civ. Eng.* **2009**, *42*, 109–113. (In Chinese)
25. Hongxin, W.; Deming, F. Mathematical Physical Model of Earth Pressure Balance Shield Tunneling and the Relationship between Parameters. *J. Civ. Eng.* **2006**, *39*, 86–90. (In Chinese)
26. Hongxin, W.; Deming, F. Earth Pressure Balance Shield Equilibrium Control Theory and Experimental Research. *J. Civ. Eng.* **2007**, *40*, 61–68. (In Chinese)
27. Lu, Q.; Fu, D. Earth Pressure Balanced Shield Tunneling Machine Cutter Torque Simulation Study. *J. Rock Mech. Eng.* **2006**, *25*, 3137–3143. (In Chinese)
28. Wei, K. Exploration of "Ideal State Soil" in Earth Pressure Balanced Shield Construction. *Urban Rail Transit Res.* **2007**, *10*, 67–70. (In Chinese)